Light front cloudy bag model: Nucleon electromagnetic form factors

Gerald A. Miller*

Department of Physics, University of Washington, Seattle, Washington 98195-1560

(Received 5 July 2002; published 3 September 2002)

The nucleon is modeled, using light front dynamics, as a relativistic system of three bound constituent quarks surrounded by a cloud of pions. The pionic cloud is important for understanding low-momentum transfer physics, especially the neutron charge radius, but the quarks are dominant at high values of Q^2. The model achieves a very good description of existing data for the four electromagnetic elastic form factors.

The recent exciting experimental results for the ratio proton elastic form factors G_E/G_M (or QF_2/F_1) [1,2] and the impending high accuracy data for the neutron electric [3] and magnetic [4] form factors have reignited interest in the venerable goal of understanding the structure of the nucleon.

The aim of the present Rapid Communication is to present a reasonable, workable model which describes currently available information and makes predictions testable against data taken at higher values of Q^2, or taken for improved accuracy. The model should have enough content so that its ultimate disagreement with experiment elucidates some missing piece of physics. Poincaré invariance and pion cloud effects, as motivated by chiral symmetry, are the principal tools used to construct the model.

Poincaré invariance is maintained or approximated by using light-front dynamics, in which fields are quantized at a fixed "time" $= \tau = x^0 + x^3 \equiv x^+$. The τ-development operator is then given by $P^0 - P^3 \equiv P^-$. The canonical spatial variable is $x^- = x^0 - x^3$, with a canonical momentum $P^+ = P^0 + P^3$. The other coordinates are $\mathbf{x}_\perp$ and $\mathbf{P}_\perp$. The relation between energy and momentum of a free particle is given by $p^- = (p_\perp^2 + m^2)/p^+$, a relativistic kinetic energy which does not contain a square root operator. This allows the separation of center of mass and relative coordinates, so that the computed wave functions are frame independent. The use of the light front is particularly relevant for calculating form factors, which are probability amplitudes for a nucleon to absorb a four momentum q and remain a nucleon. The initial and final nucleons have different total momenta. This means that the final nucleon is boosted relative to the initial one, and therefore has a different wave function. The light front technique allows one to use boosts that are independent of interactions.

We are concerned with the Dirac F_1 and Pauli F_2 [$F_2(0) = \kappa$, the anomalous magnetic moment] form factors. The Sachs form factors are $G_E = F_1 - Q^2/4M_N^2 F_2$, $G_M = F_1 + F_2$. We use the current's "good" component, J^+, so that $F_1(Q^2) = \langle N, \uparrow | J^+ | N, \uparrow \rangle$, $QF_2(Q^2) = (-2M_N) \times \langle N, \uparrow | J^+ | N, \downarrow \rangle$, with nucleon light-cone spinors, and in a frame with $q^+ = 0$ and $Q^2 = \mathbf{q}_\perp^2 = q_x^2$.

The model nucleon consists of three relativistically moving, bound constituent quarks, which are surrounded by a cloud of pions. The quark aspects [5–9], will be discussed

first. The original construction of this three-quark model was based on symmetry principles [5,6]. The wave function is antisymmetric, a function of relative momenta, independent of reference frame, and an eigenstate of the canonical spin operator. Schlumpf [7] applied it to compute a variety of baryonic properties. Frank, Jennings, and Miller [8] used this model to predict a very strong decrease of G_E/G_M as a function of Q^2, which has now been measured. Explaining the meaning of this result was left for a second paper [9] in which imposing Poincaré invariance was shown to lead to an analytic result that the ratio QF_2/F_1 is constant for large Q^2 and to a potential violation [10] of the helicity conservation rule.

The wave function we use is given by

$$\Psi(p_i) = \Phi(M_0^2)u(p_1)u(p_2)u(p_3)\psi(p_1, p_2, p_3),$$
$$p_i = \mathbf{p}_i s_i, \tau_i, \tag{1}$$

where ψ is a spin-isospin color amplitude factor, the p_i are expressed in terms of relative coordinates, the $u(p_i)$ are ordinary Dirac spinors, Φ is a spatial wave function, and the repeated indices p_i are summed over. The specific form of ψ is given in Eq. (12) of Ref. [9] and earlier in Ref. [6]. This is a relativistic version of the familiar SU(6) wave function; no configuration mixing is included. The notation is that $\mathbf{p}_i = (p_i^+, \mathbf{p}_{i\perp})$. The total momentum is $\mathbf{P} = \mathbf{p}_1 + \mathbf{p}_2 + \mathbf{p}_3$. The relative coordinates are $\xi = p_1^+/(p_1^+ + p_2^+)$, $\eta = (p_1^+ + p_2^+)/P^+$, and $\mathbf{k}_\perp = (1-\xi)\mathbf{p}_{1\perp} - \xi\mathbf{p}_{2\perp}$, $\mathbf{K}_\perp = (1-\eta)(\mathbf{p}_{1\perp} + \mathbf{p}_{2\perp}) - \eta\mathbf{p}_{3\perp}$. In computing a form factor, we take quark 3 to be the one struck by the photon. The value of $1-\eta$ is not changed ($q^+ = 0$), so only one relative momentum, $\mathbf{K}_\perp$ is changed: $\mathbf{K}_\perp' = \mathbf{K}_\perp - \eta\mathbf{q}_\perp$. We take the form of the spatial wave function from Schlumpf [7]: $\Phi(M_0) = N/(M_0^2 + \beta^2)^\gamma$, with M_0^2 is the mass-squared operator for a noninteracting system:

$$M_0^2 = \frac{K_\perp^2}{\eta(1-\eta)} + \frac{k_\perp^2 + m^2}{\eta\xi(1-\xi)} + \frac{m^2}{1-\eta}. \tag{2}$$

Schlumpf's parameters are $\beta = 0.607$ GeV, $\gamma = 3.5$, $m = 0.267$ GeV. The value of γ was chosen that $Q^4 G_M(Q^2)$ is approximately constant for $Q^2 > 4$ GeV^2 in accord with experimental data. The parameter β helps govern the values of the perp-momenta allowed by the wave function Φ and is closely related to the rms charge radius, and m is mainly
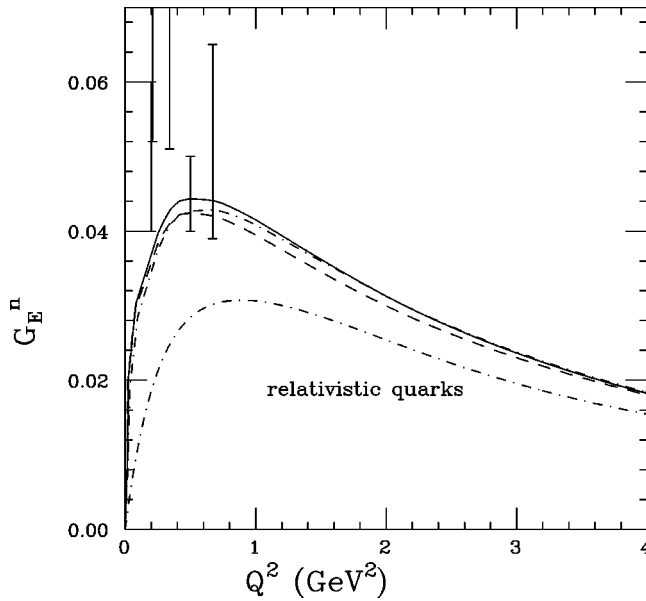
---
*Email address: miller@phys.washington.edu

FIG. 1. Calculation of G_E^n. The data are from Ref. [12].

FIG. 2. Diagrams.

determined by the magnetic moment of the proton. We shall use different values when including the pion cloud.

The calculation of form factors is simplified by using completeness to express the wave function in terms of light cone spinors $u_L(p^+, \mathbf{p}, \lambda)$, which are related to Dirac spinors by a unitary Melosh rotation evaluated in terms of Pauli spinors: $|\lambda_i\rangle, |s_i\rangle$, with $\langle\lambda_i|R_M^\dagger(\mathbf{p}_i)|s_i\rangle \equiv \bar{u}_L(\mathbf{p}_i, \lambda_i)u(\mathbf{p}_i, s_i)$. Thus the wave function depends on Melosh-rotated Pauli spinors:

$$|\uparrow \mathbf{p}_3\rangle = \left[\frac{m+(1-\eta)M_0+i\boldsymbol{\sigma}\cdot(\mathbf{n}\times\mathbf{p}_3)}{\sqrt{(m+(1-\eta)M_0)^2+p_{3\perp}^2}}\right]\binom{1}{0}, \quad (3)$$

where the quantity in brackets is $R_M^\dagger(\mathbf{p}_3)$. The function M_0 enters in the definition of the third (z) component of the quark momentum that enters in the Dirac spinors. The spin-isospin wave function can then be thought of as constructed from the nonrelativistic quark model, but with the replacement of Pauli spinors by those of Eq. (3). An important effect resides in the term $(\mathbf{n}\times\mathbf{p}_3)$ which originates from the lower components of the Dirac spinors: the orbital angular momentum $L_z \neq 0$ [11]. The term $(\mathbf{n}\times\mathbf{p}_3)$ is also responsible for the flatness of the ratio $QF_2(Q^2)/F_1(Q^2)$.

We turn now to neutron properties. The three-quark model for the proton respects charge symmetry, invariance under the interchange of u and d quarks, so it contains a prediction, shown in Fig. 1 (compared with data from Ref. [12]) for neutron form factors. We note that G_{En} would vanish in the nonrelativistic limit, $R_M \to 1$, so the deviations from 0 are solely due to relativistic effects. The resulting electric form factor, shown in the curve labeled "relativistic quarks," is very small at low values of Q^2, but at larger values of Q^2 the prediction is larger than that of the Galster parametrization [13].

The slope of G_{En} is related to the charge radius as $G_{En}(Q^2) \to -Q^2 R_n^2/6$ with a measured value [14] of R_n^2
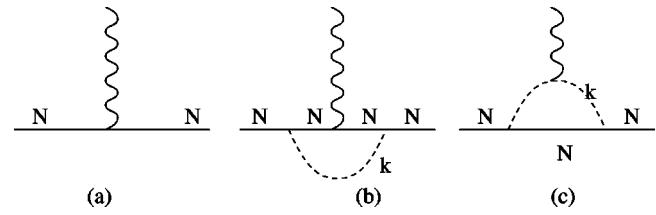
$= -0.113 \pm 0.005$ fm^2. The three-quark model value is -0.025 fm^2, obtained using Schlumpf's parameters. To understand this small magnitude we express G_E in terms of $F_{1,2}$ for small values of Q^2. Then $R_n^2 = R_1^2 + R_F^2$, where the Foldy contribution, $R_F^2 = 6\kappa_n/4M^2 = -0.111$ fm^2 is, by itself, in good agreement with the experimental data. But this does not guarantee success in explaining the charge radius because one needs to include the Q^2 dependence of F_1 which gives R_1^2. In the three-quark model $R_1^2 = +0.086$ fm^2 which nearly cancels the effects of R_F^2. Such a cancellation is a natural consequence of including the relativistic effects of the lower components of the quark Dirac spinors [15]. Another effect is needed.

Sometimes a physical nucleon can be a bare nucleon and a virtual pion. An incident photon can interact electromagnetically with a bare nucleon, Fig. 2(a), with a nucleon while a pion is present, Fig. 2(b), or with a charged pion in flight, Fig. 2(c). These effects are especially pronounced for the neutron G_E [16], at small values of Q^2, because the quark effects are small. The tail of the negatively charged pion distribution extends far out into space, causing R_n^2 to be negative. Such contributions were computed long ago using the cloudy bag model [16], which employed static nucleons.

The effects of the pion cloud need to be computed relativistically to confront data taken at large Q^2. This involves evaluating the Feynman diagrams of Fig. 2 using photon-bare-nucleon form factors from our relativistic model, and using a relativistic π-nucleon form factor. We define the resulting model as the light-front cloudy bag model LFCBM. The light-front treatment is implemented by doing the integral over the virtual pion four-momentum $k^\pm, \mathbf{k}_\perp$, performing the integral over k^- analytically, reexpressing the remaining integrals in terms of relative variables ($\alpha = k^+/P^+$), and shifting the relative $\perp$ variable to $\mathbf{L}_\perp$ to simplify the numerators. Thus the Feynman graphs, Fig. 2, are represented by a single τ-ordered diagram. The use of J^+ and the Yan identity [17] $S_F(p) = \Sigma_s u(p,s)\bar{u}(p,s)/(p^2-m^2 + i\epsilon) + \gamma^+/2p^+$ allows one to see that the nucleon current operators appearing in Fig. 2(b) act between on-mass-shell spinors.

The results can be stated as

$$F_{i\alpha}(Q^2) = Z[F_{i\alpha}^{(0)}(Q^2) + F_{ib\alpha}(Q^2) + F_{ic\alpha}(Q^2)], \quad (4)$$

where $i=1,2$ denotes the Dirac and Pauli form factors, $\alpha = n,p$ determines the identity of the nucleon, and $F_{i\alpha}^{(0)}(Q^2)$ are the form factors computed in the absence of pionic effects. The wave function renormalization constant Z is deter-

mined from the condition the charge of the proton be unity: $F_{1p}(Q^2=0)=1$. Calculating the graph of Fig. 2(b) gives

$$
F_{1bn}(Q^2) = (2F_{1p}^{(0)}(Q^2)+F_{1n}^{(0)}(Q^2))\int_N (\alpha^2 M^2 + L_\perp^2
$$

$$
-\alpha^2 Q^2/4) + (2F_{2p}^{(0)}(Q^2)
$$

$$
+F_{2n}^{(0)}(Q^2))\int_N (\alpha^2 Q^2/2), \tag{5}
$$

$$
F_{2bn}(Q^2) = (F_{1p}^{(0)}(Q^2)+F_{1n}^{(0)}(Q^2)/2)\int_N (2M^2\alpha^2)
$$

$$
+(F_{2p}^{(0)}(Q^2)+F_{2n}^{(0)}(Q^2)/2)\int_N (4\alpha^2 M^2 + 2\mu^2), \tag{6}
$$

where the integration measure $\int_N$ is given by

$$
\int_N \equiv \frac{g^2}{2(2\pi)^3}\int d^2 L_\perp \frac{d\alpha}{\alpha} R(\mathbf{L}_\perp^{(+)2},\alpha) R(\mathbf{L}_\perp^{(-)2},\alpha), \tag{7}
$$

g is the πN coupling constant, $g^2/4\pi = 14$, $\mathbf{L}_\perp^{(\pm)}\equiv \mathbf{L}_\perp \pm \alpha\mathbf{q}_\perp/2$, $\alpha D(k_\perp^2,\alpha)\equiv M^2\alpha^2 + k_\perp^2 + \mu^2(1-\alpha)$, and $R(k_\perp^2,\alpha)\equiv F_{\pi N}(k_\perp^2,\alpha)/D(k_\perp^2,\alpha)$. The πN form factor is taken as

$$
F_{\pi N}(k_\perp^2,\alpha) = \exp[-(D(k_\perp^2,\alpha)/2(1-\alpha)\Lambda^2)], \tag{8}
$$

as used by Refs. [18,19], and satisfies the constraints needed to maintain charge conservation [20]. Including the form factor this way uses the assumption that the form factor is an analytic function of k^-. The results (5), (6) show that each term in the nucleon current operator contributes to both F_1 and F_2. The evaluation of Fig. 2(c) yields

$$
F_{1cn}(Q^2) = -2F_\pi(Q^2)\int_N \frac{(1-\alpha)}{\alpha}(\alpha^2 M^2 + L_\perp^2
$$

$$
-(1-\alpha)Q^2/4), \tag{9}
$$

$$
F_{2cn}(Q^2) = -2F_\pi(Q^2)\int_N \frac{(1-\alpha)}{\alpha}(2m^2\alpha(1-\alpha)). \tag{10}
$$

The proton form factors can be obtained by simply making the replacements $n\to p$ in Eqs. (5), (6) and $-2\to +2$ in Eqs. (9), (10). The change in sign accounts for the feature that the π^- cloud of the neutron is instead a π^+ cloud of the proton.

Equations (4)–(10) completely specify the form of the calculation. But the LFCBM requires four parameters m,β,γ,Λ. Including pionic effects while continuing to use the original values of m,β,γ, would lead to a satisfactory description of G_{En} [11], but would cause other computed observables to disagree with experiment. Thus a new set of parameters is needed. The following set of requirements is used to restrict the parameters. First, the magnetic moments of the proton and neutron must agree with measured ones

TABLE I. Different parameter sets, units in terms of fm.

Set(legend)	m	β	Λ	γ	$-R_n^2$	$-\mu_n$	μ_p
1 solid	1.8	3.65	3.1	4.1	0.111	1.73	2.88
2 dot-dash	1.8	3.65	2.95	3.9	0.103	1.68	2.83
3 dash	1.7	2.65	3.1	3.7	0.109	1.79	2.95

within about 10%. We also require that the computed values of $G_{Mn}(0.5)$, $G_{En}(1,1.5)$, $G_{Mn}(4)$, $\mu G_{Ep}/G_{Mp}(5.5)$, $G_{Mp}(5.5)$, and $G_{Mp}(10)$ agree with the measured values well enough so that the average disagreement is about one error bar. Many parameter sets satisfy this criterion. We show results for three in Table I [21] and in the figures. The difference between sets 1 and 2 appears only in the value of Λ, so one can assess the dependence on that parameter.

The first application of the LFCBM is to G_{En} and the results of using the three parameters sets of Table I are shown in Fig. 1. It is easy to find many parameters which provide a large pionic effect at small values of Q^2. The agreement with existing data is good, and more higher quality data at larger values of Q^2 is expected [3]. The next step is to compute G_{Mn}, which is expressed as $G_{Mn}/\mu G_D$, where μ is the computed neutron magnetic moment and $G_D = (1 + Q^2/0.71 \text{ GeV}^2)^{-2}$. The results are shown in Fig. 3. The agreement between the present theory and existing data [22] is excellent, but this will soon be tested by a new experiment [4]. The important pionic effects can be examined by comparing the two dashed curves of Fig. 3. Neglecting the pion cloud and using the parameters of set 3, leads to a large change in the results. At high Q^2, pionic effects are absent and the difference arises from the no-pion result that $\mu_N = -1.41$ instead of -1.79. At low Q^2 the full calculation shows a dip caused by the rapid fall-off of the pion cloud contribution.

Consider the calculation of proton observables. Figure 4 shows that the measured ratio of Dirac to Pauli form factors
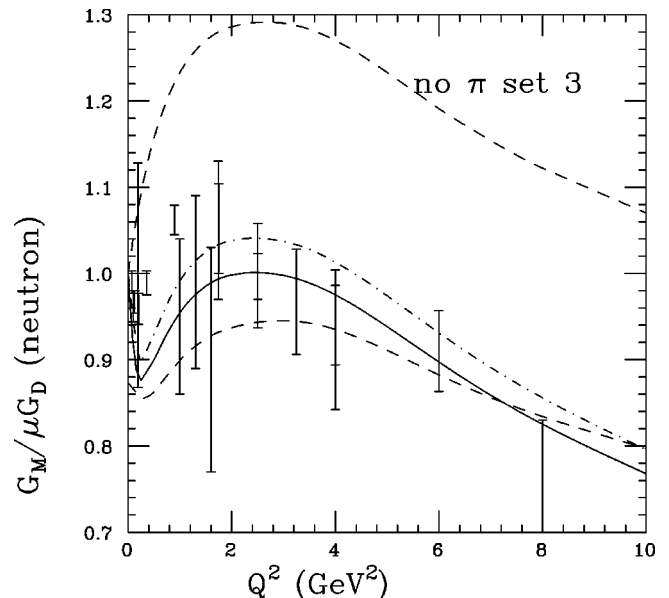

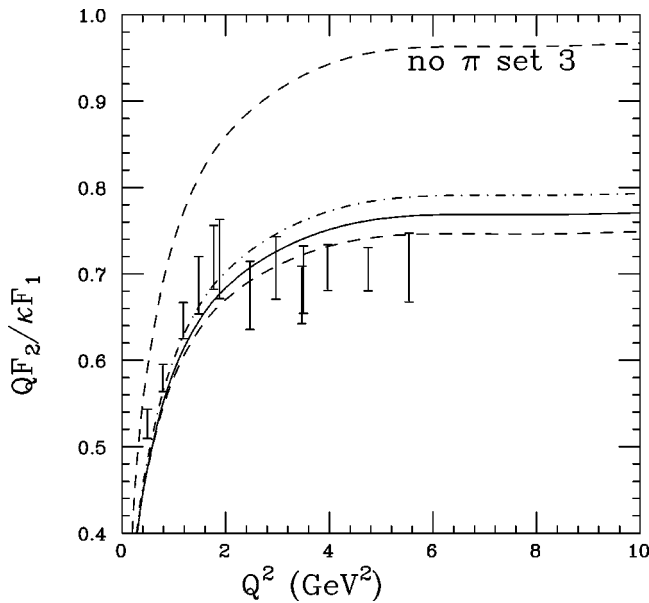FIG. 3. $G_{Mn}/\mu G_D$ for the neutron. Data are from Ref. [22].

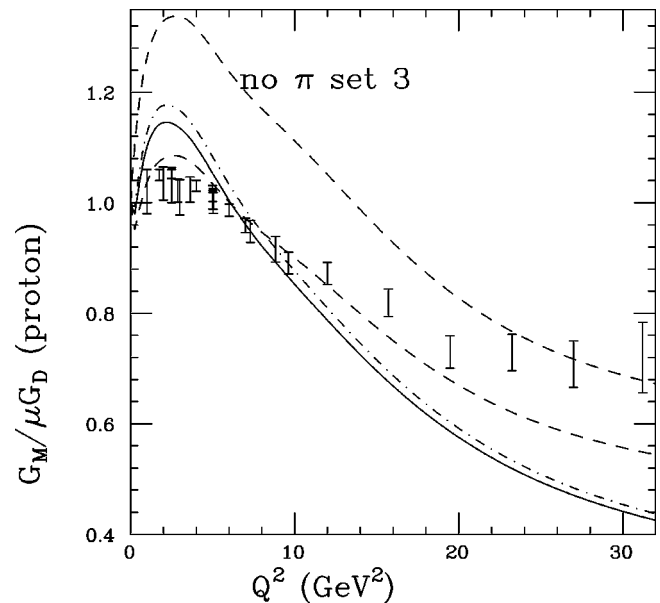FIG. 4. $QF_2/\kappa F_1$ for proton. Data are from Refs. [1,2].

FIG. 5. $G_{Mp}/\mu G_D$. Data are from Ref. [23].

is reasonably well reproduced, as we found earlier [8,9]. These ratios are not very sensitive to the parameter set. This shows that the pion cloud effects are not very important for this ratio at relatively large values of Q^2, as long as the magnetic moment is reproduced. (The effects of removing the π cloud arise mainly from the value of κ which is 1.51 instead of 1.83.) Thus, as stressed elsewhere [9] respecting symmetries is more important than including detailed dynamics in obtaining a constant ratio. Finally, the proton magnetic form factor ($G_M/\mu G_D$, where μ is the computed proton magnetic moment) is shown in Fig. 5. For this case, set 3 seems to provide a "best" description of the present data [23] up to about $Q^2=20$ GeV^2. For higher values the calculation falls a bit below the data, perhaps indicating the need for the effects of perturbative QCD. At low values of Q^2 the rapid fall-off of the π effects leads to a dip.

The axial form factor is not calculated here. Schlumpf's model obtained an excellent reproduction of existing data [7], and our parameters are similar to his. The lowest-order effect of the pion cloud vanishes, so the principal difference is that our quark masses are larger. This increases the computed value of g_A for a bare nucleon by about $10-15\%$. But this is opposed by the need to multiply the bare nucleon result by the renormalization factor Z of about $0.85-0.9$. Thus our results should be similar to those of [7].

These calculations show that the combination of Poincaré invariance and pion cloud effects is sufficient to describe the existing experimental data up to about $Q^2=20$ GeV^2. This is somewhat surprising as the model keeps only two necessary effects. Configuration mixing of quarks [24], the variation of the quark mass with Q^2 [25], exchange currents [27], and an intermediate Δ [16] have not been included. These effects either have modest influence, or are incorporated implicitly through the choice of parameters.

Perhaps the strongest model feature is that it is testable in upcoming experiments. For the proton, QF_2/F_1 is predicted to be constant for values of Q^2 up to about 20 GeV^2. The neutron G_{En}, soon to be measured, is predicted as is its magnetic form factor also soon to be measured.

There also are implications for other reactions. Hadron helicity conservation has been stated to predict that Q^2F_2/F_1 is constant [26]. This is not respected in present data, so there is no need to expect it to hold for a variety of exclusive reactions occurring at high $Q^2 \lesssim 5.5$ GeV^2. Examples include the large spin effects observed in pp elastic scattering [28] and the reaction $\gamma d \rightarrow np$ [29], but there are many other possibilities.

[1] M.K. Jones *et al.*, Phys. Rev. Lett. **84**, 1398 (2000).
[2] O. Gayou *et al.*, Phys. Rev. Lett. **88**, 092301 (2002).
[3] R. Madey, spokesperson, JLab experiment No. E93-038; D. Day, spokesperson, JLab experiment No. E93-026; B. Reitz, B. Wojtsekhowski, and G. Cates, spokespersons, JLab experiment No. E02-013.
[4] W. Brooks and M. Vineyard, JLab experiment No. E94-017.
[5] V.B. Berestetskii and M.V. Terent'ev, Sov. J. Nucl. Phys. **25**, 347 (1977).
[6] P.L. Chung and F. Coester, Phys. Rev. D **44**, 229 (1991).
[7] F. Schlumpf and U. Zurich, Ph.D. thesis, hep-ph/9211255.
[8] M.R. Frank, B.K. Jennings and G.A. Miller, Phys. Rev. C **54**, 920 (1996).
[9] G.A. Miller and M.R. Frank, Phys. Rev. C **65**, 065205 (2002).
[10] T. Gousset, B. Pire, and J.P. Ralston, Phys. Rev. D **53**, 1202 (1996).

[11] G.A. Miller, nucl-th/0206027.

[12] C. Herberg *et al.*, Eur. Phys. J. A **5**, 131 (1999); M. Ostrick *et al.*, Phys. Rev. Lett. **83**, 276 (1999); I. Passchier *et al.*, *ibid.* **82**, 4988 (1999); D. Rohe *et al.*, *ibid.* **83**, 4257 (1999); H. Zhu *et al.*, *ibid.* **87**, 081801 (2001).

[13] S. Galster *et al.*, Nucl. Phys. **B32**, 221 (1971).

[14] S. Kopecky *et al.*, Phys. Rev. Lett. **74**, 2427 (1995).

[15] N. Isgur, Phys. Rev. Lett. **83**, 272 (1999).

[16] S. Théberge, A.W. Thomas and G.A. Miller, Phys. Rev. D **22**, 2838 (1980); A.W. Thomas, S. Théberge, and G.A. Miller, *ibid.* **24**, 216 (1981); S. Théberge, G.A. Miller and A.W. Thomas, Can. J. Phys. **60**, 59 (1982); G.A. Miller, A.W. Thomas, and S. Théberge, Phys. Lett. **91B**, 192 (1980).

[17] S.J. Chang and T.M. Yan, Phys. Rev. D **7**, 1147 (1973).

[18] V.R. Zoller, Z. Phys. C **53**, 443 (1992).

[19] H. Holtmann, A. Szczurek, and J. Speth, Nucl. Phys. **A596**, 631 (1996).

[20] J. Speth and A.W. Thomas, Adv. Nucl. Phys. **24**, 83 (1997).

[21] The author will make available the computer program LFCBM.F to any researcher wishing to choose different parameters.

[22] A. Lung *et al.*, Phys. Rev. Lett. **70**, 718 (1993); S. Rock *et al.*, Phys. Rev. D **46**, 24 (1992); P.E. Bosted, Phys. Rev. C **51**, 409 (1995); R.G. Arnold *et al.*, Phys. Rev. Lett. **61**, 806 (1988); H. Gao *et al.*, Phys. Rev. C **50**, 546 (1994); W. Xu *et al.*, Phys. Rev. Lett. **85**, 2900 (2000); G. Kubon *et al.*, Phys. Lett. B **524**, 26 (2002).

[23] W. Bartel *et al.*, Nucl. Phys. **B58**, 429 (1973); A.F. Sill *et al.*, Phys. Rev. D **48**, 29 (1993); L. Andivahis *et al.*, *ibid.* **50**, 5491 (1994); R.C. Walker *et al.*, *ibid.* **49**, 5671 (1994).

[24] F. Cardarelli and S. Simula, Phys. Rev. C **62**, 065201 (2000).

[25] J.C. Bloch, C.D. Roberts, S.M. Schmidt, A. Bender, and M.R. Frank, Phys. Rev. C **60**, 062201(R) (1999); C.D. Roberts and S.M. Schmidt, Prog. Part. Nucl. Phys. **45**, S1 (2000).

[26] G.P. Lepage and S.J. Brodsky, Phys. Rev. D **22**, 2157 (1980).

[27] W.R. de Araujo, E.F. Suisso, T. Frederico, M. Beyer, and H.J. Weber, Phys. Lett. B **478**, 86 (2000); E.F. Suisso, W.R. de Araujo, T. Frederico, M. Beyer, and H.J. Weber, Nucl. Phys. **A694**, 351 (2001); K. Bodoor, H.J. Weber, T. Frederico, and M. Beyer, Mod. Phys. Lett. A **15**, 2191 (2000).

[28] E.A. Crosbie *et al.*, Phys. Rev. D **23**, 600 (1981).

[29] K. Wijesooriya *et al.*, Jefferson Lab Hall A Collaboration, Phys. Rev. Lett. **86**, 2975 (2001).